

*Citation for published version:*

Siddiq, K, Hobden, M, Watson, R, Pennock, S & Martins, S 2017, On Phase Measurement in FMCW Radar Systems. in *2017 Sensor Signal Processing for Defence Conference, SSPD 2017*. vol. 2017-January, IEEE, pp. 1-4, 7th Conference of the Sensor Signal Processing for Defence, SSPD 2017, London, UK United Kingdom, 6/12/17. <https://doi.org/10.1109/SSPD.2017.8233250>

*DOI:*

[10.1109/SSPD.2017.8233250](https://doi.org/10.1109/SSPD.2017.8233250)

*Publication date:*

2017

*Document Version*

Peer reviewed version

[Link to publication](#)

(C) 2017 IEEE. Personal use of this material is permitted. Permission from IEEE must be obtained for all other uses, including reprinting/republishing this material for advertising or promotional purposes, creating new collective works for resale or redistribution to servers or lists, or reuse of any copyrighted components of this work in other works.

**University of Bath**

## **Alternative formats**

If you require this document in an alternative format, please contact:  
[openaccess@bath.ac.uk](mailto:openaccess@bath.ac.uk)

### **General rights**

Copyright and moral rights for the publications made accessible in the public portal are retained by the authors and/or other copyright owners and it is a condition of accessing publications that users recognise and abide by the legal requirements associated with these rights.

### **Take down policy**

If you believe that this document breaches copyright please contact us providing details, and we will remove access to the work immediately and investigate your claim.

# On phase measurement in FMCW Radar Systems

Kashif Siddiq\*, Mervyn K. Hobden<sup>†</sup>, Robert J. Watson\*, Steve R. Pennock\*, Steve Martins<sup>†</sup>

\*Department of Electronic and Electrical Engineering, University of Bath, Bath, UK, BA2 7AY.

Email: {k.siddiq, r.j.watson, s.r.pennock}@bath.ac.uk

<sup>†</sup>Navtech Radar Ltd., Ardington, UK, OX12 8PD.

**Abstract**—Unlike AM and PM systems, FM systems do not necessarily require the use of a dual I/Q receiver for unambiguous phase measurement. In this paper we describe this phenomenon in detail and work out the conditions when single-channel phase measurements can be used for the reliable measurement of the phase and the Doppler frequency of targets in FMCW radars systems. The developed theory is applied to surveillance and automotive radar systems to determine the velocity bounds for the unambiguous measurement of phase. The influence of phase noise in the same context is discussed. Results of coherent averaging on the data acquired using a single-channel radar system are presented to validate the theory.

## I. INTRODUCTION

Accurate measurements of frequency and phase is central to the working of modern radar systems and are directly related to the accurate measurement of parameters like range, bearing, and velocity that are fundamental to the successful detection, tracking, and imaging, etc. of the targets of interest. In this paper we focus on the fundamental systems engineering problem of analysing simple system architectures for the reliable measurement of the phase in target returns using homodyne FMCW radar systems.

Fig. 1 shows a homodyne FMCW architecture employing in-phase (I) and quadrature (Q) mixers to demodulate the received radar signal. The instantaneous time-domain amplitude and phase can be extracted by employing this scheme. Fig. 2 shows a simpler architecture utilising a single mixer to demodulate the received signal which is then digitised and operated on by complex Fast Fourier Transform (FFT) processing. Although this method cannot be used to obtain the instantaneous phase of the received signal, we note that this is not usually required for radar applications. Post-FFT phase measurement can prove sufficient for the desired targets, and it is the purpose of this paper to analyse the conditions under which no ambiguity will occur in the phase measurement when using the system in Fig. 2. We will also demonstrate the successful application of this type of system in coherent averaging.

When the system in Fig. 2 is used, it results in a significant saving in costly hardware and engineering effort especially at microwave and millimetre wave frequencies. However this system cannot measure the negative frequency portion of the spectrum. Therefore, the system shown in Fig. 2 will measure the phase unambiguously only if the demodulated frequency spectrum is confined to one sideband. After downconversion,

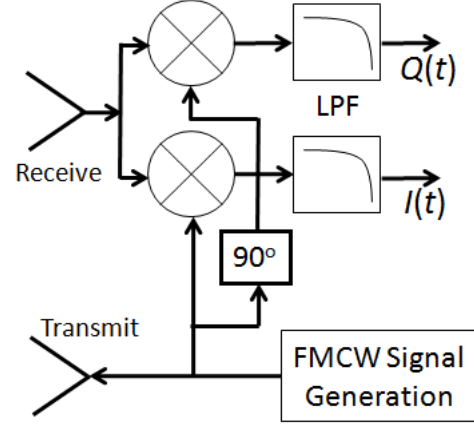


Fig. 1. Block diagram for time-domain phase measurement using an FMCW radar

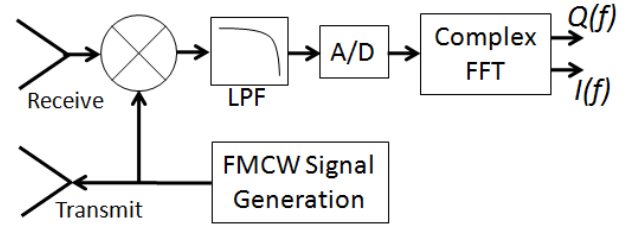


Fig. 2. Block diagram for frequency-domain phase measurement using an FMCW radar

the spectra of AM (amplitude-modulated) and PM (phase-modulated) signals are zero-centred which means that half of the modulation spectrum lies in the negative frequency region. Therefore, the I/Q demodulation scheme of Fig. 1 becomes necessary to extract the full (amplitude and phase) spectrum. In contrast FM (frequency-modulated) spectra are centred at an offset  $f_m$  from the carrier. Therefore after demodulation the baseband spectrum having bandwidth  $B$  is centred around the baseband modulation frequency  $f_m$ . If  $|f_m| - B/2 > 0$  then all the modulation power lies in only one side of the origin and the system in Fig. 2 can be used to extract the phase information in the signal unambiguously. The only cost is that the thermal noise from the image sideband will always be present, so the noise floor will be 3 dB higher than could be achieved using I/Q mixers. In the following we will analyse this phenomenon for FMCW radars.

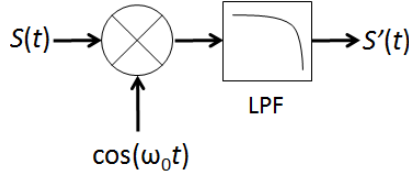


Fig. 3. Illustration of the demodulation scheme for all three types of modulation.

## II. GENERAL ANALYSIS OF MODULATED SIGNALS

In this section we mathematically analyse AM, PM and FM signals. Our analysis is motivated by [1]. Let the AM, PM and FM carrier signals be defined as below:

$$S_{AM}(t) = A_1 [1 + m_a(t)] \cos(\omega_0 t + \theta_0) \quad (1)$$

$$S_{PM}(t) = A_2 \cos(\omega_0 t + m_\theta(t) + \theta_0); |m_\theta| < 1 \quad (2)$$

$$S_{FM}(t) = A_3 \cos([\omega_0 - \omega_m]t + \theta_0), \quad (3)$$

where  $\theta_0$  represents an unknown phase shift relative to the local oscillator (LO) signal. In (3) we have considered frequency modulation resulting in a frequency translation by  $\omega_m$ . Now consider the demodulation of these signals with a LO at the carrier frequency  $\omega_0$  as illustrated in Fig. 3. The signal components in the baseband will be as follows:

$$S'_{AM}(t) = A'_1 m_a(t) \cos(\theta_0) \quad (4)$$

$$S'_{PM}(t) \approx A'_2 m_\theta(t) \sin(\theta_0) \quad (5)$$

$$S'_{FM}(t) = A'_3 \cos(\omega_m t - \theta_0). \quad (6)$$

Note that  $S'_{AM}(t)$  is scaled by  $\cos(\theta_0)$  that scales the amplitude from maximum (for  $\theta_0 = 0$ ) to zero (for  $\theta_0 = \pi/2$ ). We also notice that in  $S'_{PM}(t)$  the  $\sin(\theta_0)$  term scales the message signal from maximum (for  $\theta_0 = \pi/2$ ) to zero (for  $\theta_0 = 0$ ). In practice  $\theta_0$  varies randomly [2]. Hence, for the faithful reproduction of the AM and PM signals we need to employ the quadrature channel.

In contrast, it can be noted that  $S'_{FM}(t)$  is immune to any amplitude or phase ambiguities even in the case of employing a single channel detector. The reason is that instead of residing around the carrier (as in the case of AM and PM signals), the FM signal resides at an offset from the carrier. In other words, while the spectrum of the demodulated AM and PM signals are centred at zero frequency, the spectrum of FM signals is centred at the offset frequency  $\omega_m$ . Therefore, the full phase information can be extracted from FM signals using various signal post processing techniques, most notably the complex FFT.

In practice instead of a signal tone ( $\omega_m$  in (3)) the demodulated FM signal may contain a band of frequencies, due to signal components (like multiple targets) or due to noise components (like phase noise around a single target). For unambiguous phase measurement using a single-channel receiver, therefore, all signal and noise components must remain at a frequency offset from the carrier.

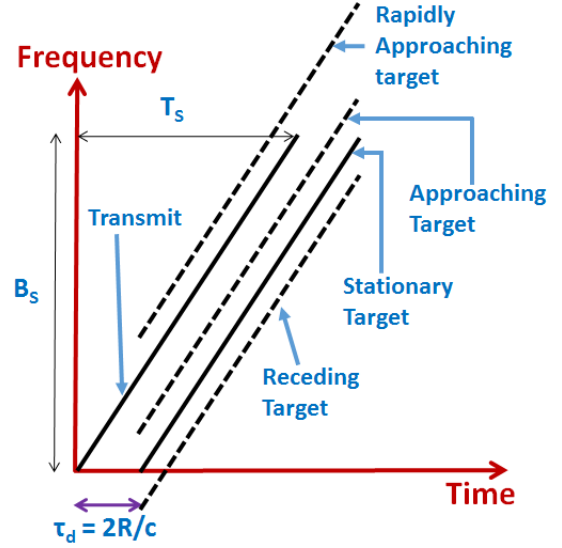


Fig. 4. Illustration of swept frequency vs time graph for a stationary, an approaching, and a receding target. The beat frequency is positive in all cases.

## III. ANALYSIS OF FMCW RADAR SIGNALS

FMCW radars use various types of waveforms and corresponding signal processing schemes to extract the range and Doppler information of the targets of interest [3]. In this section we will use the linear up-ramp signal bearing in mind that the result can be extended to other linear ramp waveforms.

Fig. 4 shows the transmit ramp as well as the receive ramps for a stationary, an approaching, and a receding target.  $B_S$  and  $T_S$  are the swept-bandwidth and sweep-time respectively.  $\tau_d$  is the round trip time delay due to a target at range  $R$ . The beat signal due to the stationary target can be written as,

$$S_{IF}(t) = A_0 \cos(2\pi f_{b0}t - \theta_0), \quad (7)$$

where,

$$|f_{b0}| = \frac{B_S}{T_S} \tau_d. \quad (8)$$

Note the similarity between (6) and (7). The Doppler shift due to an approaching target at  $R$  causes the instantaneous received frequency to be larger than that for a stationary target. The beat frequency decreases correspondingly. For a fast enough target, the Doppler shift could be large enough so that the received signal's instantaneous frequency is larger than the instantaneous transmit frequency as shown in the top plot in Fig. 4. The beat frequency will be positive in this case. One can easily extend the same arguments for a down-ramp: in that case the beat frequencies will normally be positive except for a rapidly receding target.

### A. Phase measurement in the absence of Doppler

The rapid-approaching situation in Fig. 4 cannot happen for stationary targets. Therefore it is reasonable to conclude that for stationary target detection applications, like foreign object debris (FOD) detection, the full phase spectrum can be measured unambiguously using the system in Fig. 2.

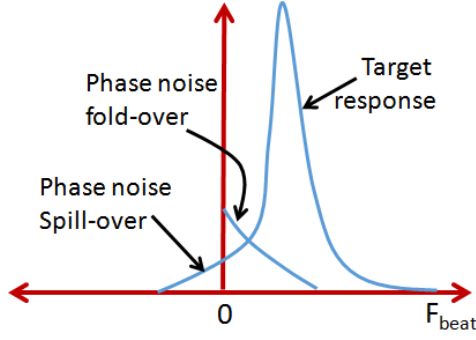


Fig. 5. Phase noise leakage in the negative frequency region.

### B. Phase measurement for moving targets

Let the beat (IF) frequency produced by the stationary target at range  $R$  be  $-f_{b0}$ . The beat frequency for an approaching target at the same range will be  $-f_{b0} + f_D$ . It follows from Fig. 4 that the beat frequency will always remain negative if  $f_D < |f_{b0}|$  (assuming an up-chirp). Therefore, for a given set of radar parameters, we can derive a relationship for the maximum allowable target velocity  $\nu$  that does not change the sign of the beat frequency as follows:

$$f_D = \frac{2\nu}{\lambda} < \frac{B_S}{T_S} \tau_d \Rightarrow \nu < \frac{\lambda B_S R}{c T_S}, \quad (9)$$

where  $\lambda$  is the carrier's wavelength and  $c$  is the speed of light. For down-ramps, (9) also sets the bound on the maximum velocity receding targets could have without changing the sign of the beat frequency. Thus for triangular sweeps (9) sets the dynamic range of allowable velocities that would result in unambiguous phase measurement.

From (9) it is apparent that the velocity dynamic range can be increased by reducing the Doppler frequency relative to the beat frequency of a given target. This can be done by increasing  $\lambda$  and/or increasing the sweep rate  $B_S/T_S$ .

### C. Effect of phase noise

Phase noise appears as noise sidebands on the target response. When the target is very close in range some of the noise sidebands can spread into the negative frequency region. When using the single-channel receiver of Fig. 2 the negative frequency portion of the target spectrum would wrap around and appear as increased noise in the positive frequency region. This is illustrated in Fig. 5.

However it is known that for close ranges the phase noise decorrelates heavily so that the noise sidebands are minimised [4]. For short ranges, the phase noise is decorrelated as 20 dB/decade [4], so if the target's spectrum is steeper than -20 dB/decade there will be residual phase noise that can spill-over and then fold-over. This can happen when a large target is close to the radar.

This effect can be even more pronounced when the target is at a farther range but the target peak appears at a lower frequency due to Doppler shift. The phase noise decorrelation (i.e. the difference in the transmitted and received phase noise

TABLE I  
PARAMETERS OF EXAMPLE RADARS

Parameters	Surveillance	Automotive
Carrier Frequency	76.5 GHz	24 GHz
Carrier Wavelength	3.9216 mm	12.5 mm
Sweep Time $T_S$	2 ms	1 ms
Coherent Processing Interval (CPI)	2 ms	64 ms
Doppler Resolution, $1/CPI$	500 Hz	15.625 Hz
Velocity Resolution, $\lambda/(2CPI)$	0.98 m/s	0.0977 m/s
Swept Bandwidth $B_S$	600 MHz	150 MHz
Doppler Shift at 1 m/s	510 Hz	160 Hz

TABLE II  
MAXIMUM VELOCITY FOR UNAMBIGUOUS PHASE MEASUREMENT

Range	Surveillance		Automotive	
	m/s	mph	m/s	mph
1 m	3.92	8.77	6.25	14
10 m	39.2	87.7	62.5	140
100 m	392	877	625	1400

processes) will essentially be according to the target's actual range. Detailed calculations of the effect must be carried out using the detailed phase noise spectra. This problem can also be alleviated if  $\lambda$  and/or the sweep rate is increased as explained above.

## IV. APPLICATION TO FMCW RADAR SYSTEMS

### A. Maximum velocity calculations

The application of (9) to radar systems is straightforward. Table I shows the parameters of a surveillance radar and an automotive radar. Table II shows the maximum permitted velocities calculated using (9) for targets at various ranges. It is apparent that in most practical situations the target velocities are under these limits. This is a strong result that suggests that a single-channel demodulator followed by complex FFT processing can be used for coherent processing and phase measurement in a wide variety of situations. For lower carrier frequencies the requirement for the maximum velocities is even more relaxed as evidenced by this example.

### B. Effect on Range-Doppler algorithms

FMCW radars employ various waveforms to extract the true range and Doppler information from radar signals. These include triangular sweeps, the chirp sequence waveform, the multiple FSK waveform, and the intertwined chirp sequence waveform [3]. In general the triangular sweep will have the Doppler limit of (9) on both the up-sweep and the down-sweep (i.e. approaching as well as receding targets). Other waveforms employing only the up-ramp or the down-ramp respectively will have the Doppler limit for approaching or receding targets only.

## V. MEASUREMENT RESULTS FROM A PRACTICAL FMCW RADAR SYSTEM

In this section we present the results of coherent averaging performed on signals measured using the 76.5 GHz surveil-

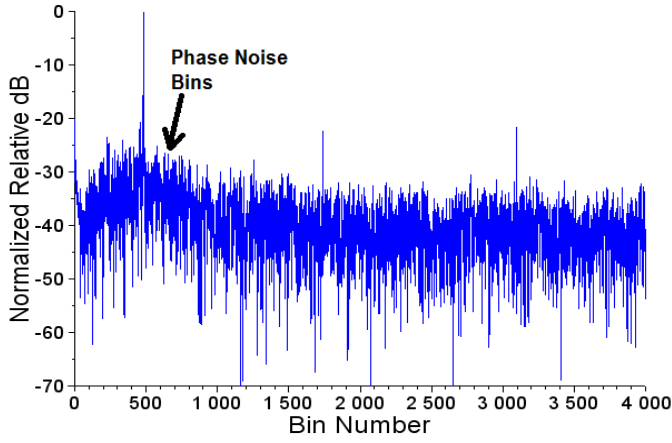


Fig. 6. Radar scene display from a single FMCW sweep. Three target peaks are visible. The bins size is 25 cm.

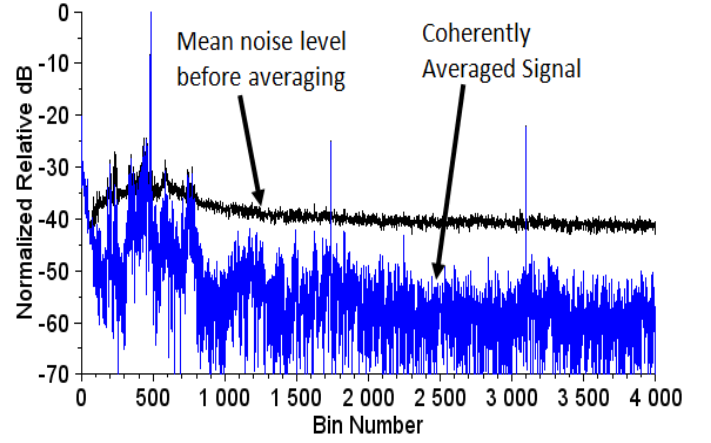


Fig. 8. Improvement in SNR due to coherent averaging. The mean noise level before averaging is also displayed for comparison.

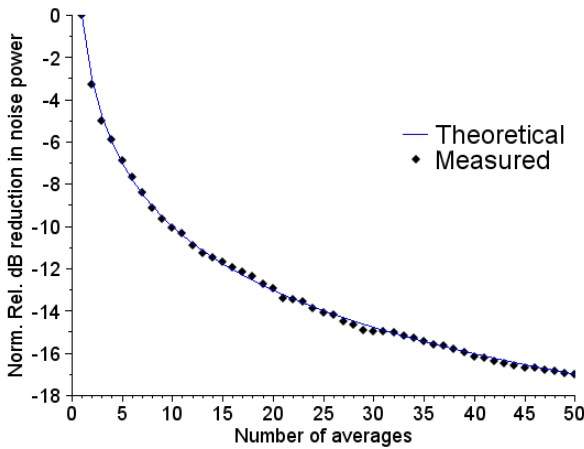


Fig. 7. Variation of noise power with averaging

lance radar system of Table I based on Fig. 2. If the phase is measured faithfully using the system in Fig. 2 then coherent averaging should result in  $N$ -times improvement in the SNR, where  $N$  is the number of signal records being averaged [5].

A raw display of the scene being analysed is shown in Fig. 6. Three target peaks can be seen along with the raised noise floor due to phase noise around them. The bins displayed in the abscissa are 25 cm each. The ordinate is normalized to the highest signal in the scene. The dB units are arbitrary in that they are not relative to any common reference (this is a common way of displaying range-profiles in radar systems).

50 sweeps of complex radar data from this scene were recorded and the coherent average was computed. First the phase noise bins shown in Fig. 6 were analysed. The dotted line in Fig. 7 shows the decrease in noise power versus an increasing number of averages by varying  $N$  from 1 to 50. The result has been normalised to the noise power when  $N = 1$ . The solid line is a plot of the function  $1/N$  on the semi-log scale. The result shows an agreement with the theoretical

prediction of the improvement in SNR.

In Fig. 8 the coherently averaged data has been plotted, along with the mean noise level from Fig. 6 (i.e. without averaging). The improvement in SNR as well as the phase noise sidebands is apparent which leads to better definition in the scene.

## VI. CONCLUSION

In this work we analysed the effectiveness of the FMCW radar architecture employing only a single channel detector followed by complex FFT processing to extract the phase information. A mathematical analysis of various modulation schemes was presented to give the idea a strong theoretical foundation. It was found that the said radar architecture successfully measures the phase information for static targets. For moving targets a maximum velocity condition was derived for unambiguous phase measurement. Practical examples demonstrated that this condition is easily met in a wide variety of applications. Coherent averaging performed on measurements from a surveillance FMCW radar system shows an improvement in SNR according to the theoretical prediction, signifying reliable phase measurement.

## ACKNOWLEDGMENT

This work was partially supported by Innovate UK.

## REFERENCES

- [1] D. G. Tucker, "The synchrodyne and coherent detectors," *Wireless Engineer*, July 1952.
- [2] S. Haykin, *Communication systems*, 4th ed. John Wiley & Sons, 2001.
- [3] M. Kronauge and H. Rohling, "New chirp sequence radar waveform," *Aerospace and Electronic Systems, IEEE Transactions on*, vol. 50, no. 4, pp. 2870–2877, October 2014.
- [4] K. Siddiq, R. J. Watson *et al.*, "Phase noise analysis in FMCW radar systems," *12th European Radar Conference (EuRAD)*, pp. 501–504, Sept 2015.
- [5] M. A. Richards, *Fundamentals of radar signal processing*. McGraw-Hill, 2005.